J. COMBIN. MATH. COMBIN. COMPUT. 127b (2025) 3825--3845

Journal of Combinatorial Mathematics
and Combinatorial Computing
www.combinatorialpress.com/jcmcc

Applying Principal Component Analysis to Optimize Visual Effects and Information Communication in Visualization Designs

Jun Wang[1,✉]

[1] College of Cultural Creativity and Tourism, Yuncheng Vocational and Technical University, Yuncheng, Shanxi, 044000, China

ABSTRACT

Visual communication design requires that feeling information and exchange of information must be conveyed efficiently and accurately. In this paper, we design a robust principal component sub-analysis visual enhancement algorithm based on improved Retinex. The algorithm transforms the image to the logarithmic domain so that it satisfies the decomposition condition of RPCA. After the RPCA decomposition model to get the low-rank component and sparse component, and will use adaptive gamma correction algorithm for the low-rank component for contrast enhancement, the two components are combined and then inverse transformed in the logarithmic domain to get the enhancement results. To avoid color distortion, the input image is converted to HSV color space to separate illumination information from noise. The model uses the inexact augmented Lagrange multiplier method (IALM) to solve the optimization problem, which leads to a significant improvement in the decomposition speed. The performance of the designed algorithm is verified on the dataset, and it is found that after the color equalization process for overexposed images, the gray value distribution is more uniform, and the image shows a better sense of brightness and visual effect after the contrast is increased. The algorithm scores 0.4648 and 0.7577 in UCIQE and UIQM respectively, which are ranked first among all algorithms and have better visual effect and information communication efficiency.

Keywords: retinex, color balance, principal component analysis, image enhancement, visual design

1. Introduction

Visual design is the process of communicating information using visual elements and user experience. Its definition emphasizes the importance of the use of visual elements, user experience, and communication of information [1-2]. Through visual design, it is possible to create attractive, easy to

✉ Corresponding author.
E-mail address: ww2011522@163.com (J. Wang).
Received 10 June 2024; Revised 25 August 2024; Accepted 20 January 2025; Published Online 16 April 2025.
DOI: 10.61091/jcmcc127b-213

understand, and impressive visuals that enable better communication of information and provide a better user experience [3-4]. It specifically includes social media visualization, visual expression, data visualization, graphic design and user experience design [5]. Currently visualization design research continues to develop at home and abroad and covers a wider range of fields, and research related to visualization design has become a hot spot.

With the rapid development of computer network, the visualization pathway of Internet information becomes richer and richer, and in the field of visual communication and design, in addition to the traditional text, image and animation, the communication of visual information mainly relies on the graphic elements in the visualization interface [6-8]. Taking webpage design as an example, webpage is a collection of all kinds of visual elements, and the design of key visual elements such as color, image and text within the webpage needs to follow the basic rules of visual communication and pay attention to the impact of visual information and the humanized construction of human-computer interaction environment [9-10].

In the traditional way of designing the visual communication of Internet information, the user's cognitive psychology is generally taken as the basis of design, and less attention is paid to the emotional communication and content interaction between the visual elements and the users, which leads to the fact that the users only take the App interface and webpage content as the entrance to obtain information, and neglect the value of the information carrier itself [11-13]. Information graphic interaction technology is a personalized visual element technology means based on graphic beautification technology, aiming to enhance the user's attention to the information of visual elements by enhancing the graphic interactivity in the design of visual elements, which in turn enhances the effect of graphic visual expression [14-16]. As an important medium for information visual communication, information graphics are significantly different from ordinary decorative graphics, which present different forms such as icons, UI, and guide symbols in different apps, web pages, and other interface designs, and have the role of information transmission [17-19].

For interface design, the communication of visual information mainly relies on coding and decoding conversion, in which the designer of the interface encodes the initial information data that the webpage needs to carry as the visual language, and then through the decoding process on the user's side, the design elements in the visual language are converted into information that is easy to be accepted by the user [20-22]. The interaction process between the designer and the interface is the process of transforming the initial data to visual information, and the interaction process between the user and the interface is the process of transforming the visual information into the knowledge they have learned, so the process of information graphicalization can be regarded as the practical application of coding and decoding theory in semiotics [23-25]. Using the graphics of the interactive interface, the designer can take the organization and processing of the initial data as the basis of the graphical interaction, and precisely define the user's interface interaction actions to complete the communication, transformation and reception of important visual information. At the user's end, the user's information reception belongs to the process of “decoding” after decoding, where the user visually translates the information contained in the graphic according to his own cognitive style and comprehension ability, and selectively receives the information content after the emergence of mental activities [26-28]. It can be seen that the information graphics in the interactive process plays a leading role, reasonable application of graphical interaction technology can stimulate the interest of users and assist them to complete the efficient identification of information.

Exploring the underlying logical issues in visualization practices and applications in related research, literature [29] tested and evaluated the presentation of different visual effects of VHs colliding with the real physical world, indicating that visual effects exerted an influence on user socialization, interaction, and physical states based on different scenarios and effect types. Literature [30] conducted a comparative survey experiment and indicated that student textbook choices are attributed to the visual design image of the textbook and the students' perception of the textbook impression, which provides an important reference for personalizing the visual design of textbooks. Literature [31] in the study of smartphone interface indicated that the visual design of icon color and border shape significantly affects the user's search efficiency and cognition, and the optimization related to visual design can improve the user experience. Based on the stimulus-organism-response theory, literature [32] illuminated the complexity of background visualization design of live broadcasting room, which can stimulate consumers' purchasing desire by inducing and guiding customers' emotions, in which the complexity of background visualization design and consumers' emotions present an inverted U-shaped relationship.

In the design innovation category of research around the optimization of visual design technology work, literature [33] envisioned a three-path mediation model to evaluate website visual design metrics, which was found to have a positive effect on website visual evaluation through its effect on usability and pleasantness. Literature [34] designed a visualization framework for collaboration with seven features such as structural constraints for identifying visualizations, content modifiability, etc., which effectively supports designers in visualization design. Literature [35] attempted to use an automated intelligent model to assess and predict the relative importance of visualization and image design elements, and verified the feasibility based on simulation experiments. Literature [36] conceived a method for automatic extraction of stylistic information for image design with a series of character detection, style classification and clustering techniques as the core technology, which can effectively identify and predict the visualization of image problems and typographic design trends. Literature [37] conceived an ontological framework to optimize the visual analysis (VA) process for impediments such as technical deficiencies and to effectively support developers in visual visual analysis and design in a structured and systematic manner.

In this paper, Retinex is first optimized to convert color images into HSI spatial model with adaptive stretching of saturation. A convolution operation is performed using bootstrap filtering to estimate the incident component of the image and enhance the real visual brightness. Then for the shortcomings of the global lookup table method, an ACE acceleration algorithm based on local linear lookup table (LLLUT) is proposed, which can ensure the color intelligent optimization quality of the output image while accelerating the algorithm. The image is decomposed into a low-rank component containing illumination information and a sparse component containing noise and detail information to improve the robustness of the decomposition model to interference information. For the illuminance component, an adaptive gamma correction algorithm is used for contrast enhancement to realize the adaptive capability. Finally, the two components are combined to obtain the enhancement results.

2. Visual Enhancement Algorithm for Principal Component Sub-Analysis Based on Improved Retinex

2.1. The retino-cortical theory

The retina-cortex (Retinex) theory is an image generation theory based on the visual properties of the human eye. The theory considers that an image consists of two components, the illuminance component and the reflection component, as shown in equation (1).

$$I = L * R \tag{1}$$

where: I is the original image; L and R represent the illumination and reflection components respectively; $*$ represents the corresponding pixel multiplication. The illumination component characterizes the structural information and illumination information of the image, which belongs to the low-frequency component: the reflection component characterizes the detail information and noise of the image, which belongs to the high-frequency component.

Based on the above theory, Retinex image enhancement model is proposed, and the block diagram of the model is shown in Fig. 1.

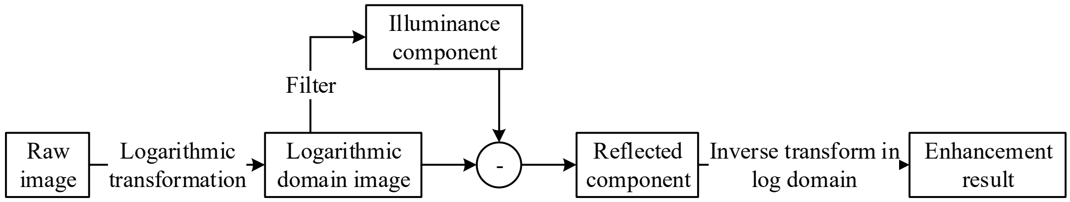

Fig. 1. Block diagram of Retinex model

The model first transforms the image to the logarithmic domain by transforming Eq. (1) to a logarithmic domain expression as shown in Eq. (2).

$$\log I = \log L + \log R \tag{2}$$

A Gaussian filter is then utilized to obtain the estimated illuminance component, shifting the term of equation (2) to obtain the reflection component in the logarithmic domain, which is reduced from the logarithmic domain and gives the final enhancement result.

2.2. Improvement of the Retinex algorithm

2.2.1. Saturation component of an adaptively stretched image. The traditional Retinex algorithm enhances the R,G,B-component of the color image, which is easy to destroy the memory connection between the R,G,B-components, for this reason, the color image is first converted into the HSI spatial model, in which H,S,I describes the hue, saturation and brightness of the color, respectively [38]. Where saturation mainly describes the depth of the image color as (3).

$$S = 1 - \frac{3}{R+G+B}[\min(R,G,B)] \tag{3}$$

When the lighting conditions are not so good, the value of S is relatively small, for this reason, the saturation needs to be adaptively stretched as in equation (4);

$$\tilde{S} = \left(1 + \frac{M_V}{\max(R,G,B) + \min(R,G,B) + 1}\right)S \tag{4}$$

where M_V represents the saturation principal mean of the color image.

2.2.2. Enhancement of image brightness. In low illumination conditions, the luminance of the color image is compared, for this reason a bootstrap filter is used to perform a convolution operation with the original to estimate the incident component of the image. The bootstrap filter can be expressed as equation (5).

$$q_j = a_k I_j + b_k \tag{5}$$

Let the estimated value of the reflection component of the image be $\tilde{R}_i(x,y)$. The luminance of the image is processed using the gamma correction algorithm, which is specified in equation (6).

$$R_{vi}(x,y) = (\tilde{R}_i(x,y))^{1/\gamma} \tag{6}$$

where γ is the correction parameter.

The luminance component after image enhancement is Eq. (7).

$$I_{enhanced} = R_v(x,y) = \sum_{i=1}^{3} W_i R_{vi}(x,y) \tag{7}$$

where $W_i, i = 1,2,3$ denotes the weights of the 3 scales, i.e., the weight coefficients of the 3 luminance levels of the image, i.e., low, medium, and high.

2.2.3. Color recovery process. After the image enhancement process, the image color may be distorted, so the image color recovery process is required. The color recovery function is equation (8).

$$C_i(x,y) = G_n \ln\left[\frac{\alpha G_i(x,y)}{\sum_{i=1}^{3} G_i(x,y) + \beta + 1}\right] \tag{8}$$

where, G_a represents the gain parameter; α represents the degree of image adjustment brightness, and β represents the degree of adjustment image color scheduling.

The color channel after color recovery is equation (9).

$$\tilde{G}_i(x,y) = C_i(x,y) g_i(x,y) \tag{9}$$

The workflow based on the improved Retinex algorithm is shown in Fig. 2.

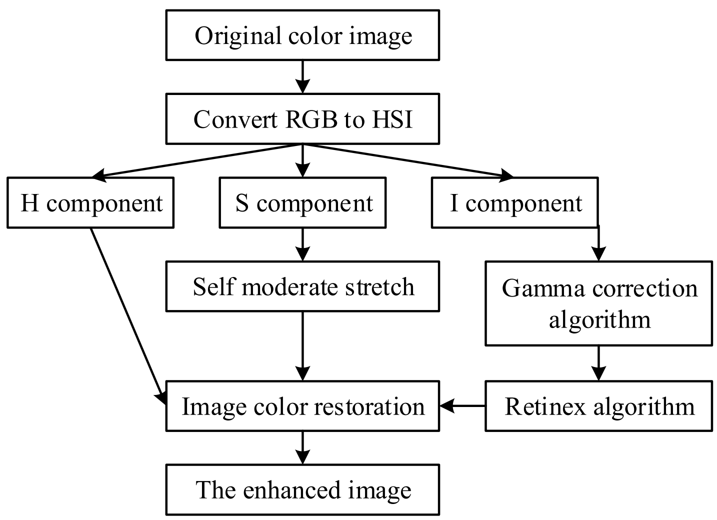

Fig. 2. Workflow of the improved Retinex algorithm

2.3. Color balance optimization for visual effects

2.3.1. Automatic Color Equalization. Automatic Color Equalization (ACE) algorithm is a color processing algorithm based on the characteristics of the human visual system to process the original image with excellent color correction effect, which can improve the color defects existing in the original image and the local and overall contrast, and improve the color saturation of the image, and then enhance the visual effect of the image [39]. Its basic process is shown in Figure 3.

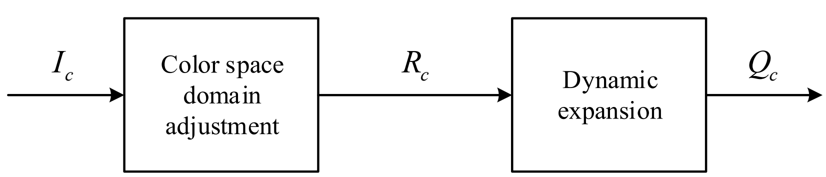

Fig. 3. Processing flow of automatic color balancing algorithm

As can be seen from the figure, the processing flow of the automatic color equalization (ACE) algorithm for image color correction is mainly divided into two parts, the first part is to achieve chromatic aberration correction by adjusting the color or spatial domain of the image, and to obtain the reconstructed image of the null domain; the second part is to dynamically expand the final output image. The automatic color equalization (ACE) algorithm is implemented by imitating the "side suppression" extreme to adjust the color/spatial domain of the image, to obtain the relationship between the original input image and the final output image, and its calculation formula can be expressed as follows:

$$R_c(p)=\sum_{j\in Sabsel, j\neq p}\frac{r(I_c(p)-I_c(j))}{d(p,j)} \tag{10}$$

where, $R_{ò}$ represents the final output image; $I_{ò}$ represents the original input image; represents the subset of pixels involved in the operation; p represents the current pixel point in the image, j represents the reference pixel point, $I_c(p)-I_c(j)$ represents the difference in the brightness of the two pixels; r represents the difference in the relative brightness between a pixel point and its other similar points around it as a singular function; d represents the distance between the two pixels as a function of the height, and adopts the Manhattan distance as the d function whose formula can be expressed as:

$$d(i,j)=|x1-x2|+|y1-y2| \tag{11}$$

where $(x1,y1)$ and $(x2,y2)$ represent coordinate point i and coordinate point j respectively, and $d(i,j)$ represents the Manhattan distance between the two coordinate points.

Considering that the saturation function is better for color correction in the case of having most conditions, this is used as the r function, and its calculation formula can be expressed as:

$$r(x)=\begin{cases}-1, x<-T\\ x/Slope, -T\leq x\leq T\\ 1, x>T\end{cases} \tag{12}$$

where T represents the saturation threshold, $T=20$; $Slope$ represents the slope, $Slope=1/20$.

2.3.2. LLLUT-based ACE optimization algorithm. The traditional ACE algorithm has the advantages of excellent dynamic performance, good retention of local features and details, and is one of the most commonly used color correction algorithms, but the ACE algorithm has the disadvantage that as the image size needs to be adjusted is getting bigger and bigger, its computational complexity is getting higher and higher and the computation time is getting longer and longer, and some of them may take a number of hours or even longer.

The purpose of optimizing the ACE algorithm is to reduce its computational complexity, improve the speed performance of the algorithm for image equalization processing, and select the local linear lookup table (LLLUT) method to optimize the ACE algorithm. The specific optimization method is to introduce a reduction factor in the ACE algorithm, reduce the original image, and then use the ACE algorithm to automatically color balance the reduced image; after that, according to the local linear transformation rules to restore the processed reduced image to obtain the final corrected image, to achieve the purpose of improving the visual effect of the image.

The specific realization steps are as follows:

1) Set, the original input image as I and the subsampling factor as d^2. After subsampling the original image using the sampling factor, a thumbnail image I^* is obtained;

2) Perform a color equalization operation on the thumbnail image using an automatic color equalization (ACE) algorithm to obtain a thumbnail image O^*;

3) For each color channel in the image, a separate LUT function is constructed to continuously pass close to a multi-valued function capable of mapping pixel values from the pixel values of the thumbnail image I^* to the pixel values of the thumbnail image O^*, which has been processed by the automatic color equalization (ACE) algorithm;

4) Applying the LUT function built in step 3 to the original input image I, and finally outputting the reduced-size filtered image O_{LUT}.

The formula for the global lookup table method can be expressed as:

$$O_{LUT} = LUT(I, I^*, O^*) \tag{13}$$

The basic principle of the local linear lookup table (LLLUT) algorithm is to consider the position of the pixel points in the image, i.e., according to the pixel value of a specific image flocculation point in the original input image, and the pixel value of the pixel point corresponding to it in the thumbnail image, and in the thumbnail image after the automatic color equalization processing to build the LLLUT function, to make up for the deficiencies that exist in the global lookup table method.

The formula of LLLUT algorithm can be expressed as:

$$O_{LLL}(x,y) = LLL_{(x,y)}(I_{(x,y)}, I_{\Omega}^{S}, O_{\Omega}^{S}) \tag{14}$$

The implementation steps of the ACE optimization algorithm based on LLLUT are as follows:

1) Divide the original input image I into L square sub-matrix blocks with d value as the side length, calculate the average of all pixel values in each sub-matrix block, and use the result of the calculation as a substitution point for that sub-matrix block. A smaller thumbnail I^* is obtained by combining all the substitution points;

2) Perform an automatic color equalization calculation operation on the thumbnail I^* using the ACE algorithm and input the corrected thumbnail image O^*

3) According to the local linear transformation rule, restore the low-resolution thumbnail image O^* to the original input image I resolution, and obtain the final output image O_{LLLUT}.

Wherein, the local linear transformation rules are as follows:

1) Let, the position coordinate of each pixel point in the channel c of the original input image I be $(x,y) \in I_c$, and the position coordinate (x_i, y_i) corresponding to that pixel point in the thumbnail images I^* and O^* is calculated, which can be expressed as:

$$(x_s, y_s) = (\mathrm{int}(\frac{x}{d}) \cdot \mathrm{int}(\frac{y}{d})) \tag{15}$$

2) According to the position coordinates of the pixel point (x_s, y_s) with this coordinate point in the thumbnail image I^* up and down, left and right a total of 5 points for the definition of the region, its calculation formula can be expressed as:

$$5N(x_s, y_s) = \begin{Bmatrix} (x_s, y_s), (x_s+1, y_s), (x_s-1, y_s), \\ (x_s, y_s+1), (x_s, y_s-1) \end{Bmatrix} \tag{16}$$

$$\Omega_{\mathrm{center}} = 5N(x_s, y_s) \tag{17}$$

Where, Ω_{center} represents the defined region of pixel point position coordinates (x_s, y_s), the main role of this region is to solve the information interpolation required when the local linear mapping function is determined.

3) Let, the existence of pixel points (x_i, y_i) and $(x, y,)$ in each defined region can minimize the value of the defined non-negative parameter, the specific formula is as follows:

$$\Delta_t = I_c(x,y) - I_c^s(x_t, y_t) \tag{18}$$

$$\Delta_r = I_c^s(x_r, y_r) - I_c(x,y) \tag{19}$$

When $\Delta_i \geq 0, \Delta, \geq 0$, $I_{\mathrm{o}}^{*}(x, y,)$ represents the minimum value greater than $I_c(x,y)$, which is the approximate pixel value around the $I_c(x,y)$-position coordinates;

4) Let:

$$p_l = I_c^s(x_l, y_l), p_r = I_c^s(x_r, y_r) \tag{20}$$

$$q_l = O_c^t(x_l, y_l), q_r = Q_c^*(x_r, y_r) \tag{21}$$

If point (x_r, y_r) does not exist, let $p_r = 255, q_r = 255$; if point (x_t, y_t) does not exist, let $p_t = 0, q_t = 0$.

5) Define the linear LUT as line segment $L(x, y) = \{(p_t, q_t), (p_r, q_r)\}$ and finally solve for $O_{\delta}(x, y)$ based on the linear function with $I_c(x, y)$ positional coordinates.

2.4. Adaptive enhancement algorithm based on robust principal component analysis

Based on the above visual effect enhancement design, this section designs an adaptive enhancement algorithm based on robust principal component analysis (RPCA). Through RPCA decomposition, the proposed algorithm can accurately separate illumination information from noise for images in different lighting environments, thus avoiding noise amplification.

2.4.1. Robust principal component analysis. Robust Principal Component Analysis (RPCA) is chosen for image decomposition.RPCA is based on PCA by introducing sparsity of noise, which makes the decomposition method more robust to noise with large amplitude [40].RPCA considers that a matrix can be composed of a low-rank matrix and a sparse matrix, i.e., a low-rank component and a sparse component as shown in Eq. (22).

$$X = A + E \tag{22}$$

In image decomposition, X is the input image, and A and E represent the low-rank and sparse components, respectively. Where the smaller rank makes the sample features in the low-rank component have strong correlation, which can be characterized as illumination information; the features in the corresponding sparse component have stronger independence, which can be characterized as detail texture information and noise. In order to solve the above two components, the constrained optimization problem can be obtained according to Eq. (22), as shown in Eq. (23).

$$\min_{A,E}\left(rank(A) + \lambda \| E \|_0\right) \quad s.t. X = A + E \tag{23}$$

where $rank(\cdot)$ represents the rank of the matrix to be solved and $\|\cdot\|_0$ represents the 0-parameter of the matrix. λ is the weight coefficient, which serves to balance the weights of the two components. When the weight coefficient is large, the low-rank component obtained by RPCA decomposition has more complete structural information, but may contain some noise. When the weight coefficient is small, the low-rank component obtained by RPCA decomposition is smoother and less noisy, but the sparse component will have more detailed information mixed with noise.

An equivalent transformation of Eq. (23) is performed by replacing the rank of the matrix with the kernel paradigm and the 0-parameter with the 1-parameter, thus converting the NPHard problem into a relaxed convex optimization problem, as shown in Eq. (24).

$$\min_{A,E}(\| A \|_* + \lambda \| E \|_1) \quad s.t. X = A + E \tag{24}$$

where $\|\cdot\|_*$, represents the kernel paradigm of the matrix and $\|\cdot\|_1$ represents the 1-parameter of the matrix. The image is transformed to the logarithmic domain for RPCA decomposition according to the Retinex enhancement model as shown in Eq. (25).

$$\min_{A,E}(\| A \|_* + \lambda \| E \|_1) \quad s.t. \tilde{I} = A + E \tag{25}$$

where $\tilde{I}, A, E$ represents the original image, the low-rank component and the sparse component of the log domain, respectively.

2.4.2. Optimization problem solving. Augmented Lagrange multiplier method (ALM) is a classical and efficient optimization method, which introduces the idea of pairwise ascent method on the basis of the traditional Lagrange multiplier method to make the problem have the nature of convex function.ALM has a greater advantage in solving optimization problems with equational constraints.

The form of the augmented Lagrange multiplier method is shown in (26).

$$\min f(x) \quad st.\varphi(x)=0 \tag{26}$$

$$L(x,\lambda)=f(x)+\lambda\varphi(x)+\frac{\rho}{2}\|\varphi(x)\|_2^2 \tag{27}$$

where λ is the weight coefficient in the Lagrange multiplier method, $\frac{\rho}{2}\|\varphi(x)\|_2^2$ is the penalty term in the augmented Lagrange multiplier method, and ρ is the penalty factor. The augmented Lagrange function for RPCA decomposition is obtained:

$$L(A,E,Y,\rho)=\|A\|_*+\lambda\|E\|_1+\langle Y,\tilde{I}-A-E\rangle+\frac{\rho}{2}\|\tilde{I}-A-E\|_2^2 \tag{28}$$

where Y is the Lagrangian weight matrix and ρ is the penalty factor. When the derivative of Eqs. (4-9) is zero, the corresponding matrix A,E is the desired low-rank and sparse matrix. In order to improve the computational efficiency of the algorithm, the proposed algorithm uses the inexact increasing-plant Lagrange multiplier method (IALM) to solve the optimization problem of the model.

2.4.3. Image enhancement. In order to achieve the purpose of bright color separation, the proposed algorithm converts the input image to HSV color space. Since the HSV model describes the visual properties of the human eye, it is more suitable for describing the color characteristics of an image, and it has a greater advantage in dealing with the luminance information of low-light images [41]. There are three parameters in this model which are hue (H), saturation (S) and illumination (V).

The hue represents the spectrum of the image, different colors have different spectra, in the model with the size of the angle that it ranges from $[0°,360°]$, where $0°$ represents red, $180°$ represents cyan; saturation represents the degree of mixing of a certain color with white, the higher the saturation, the more vibrant the image color, the model with the distance from the center of the circle, which ranges from [0, 1], the greater the value indicates that the higher the degree of saturation; illuminance Indicates the brightness of a certain color, expressed in the model by the vertical distance from the apex of the cone to the plane, which ranges from [0, 1], the larger the value, the higher the image brightness.

$$\begin{gathered}
V_{\max}=\max(R,G,B) \quad V_{\min}=\min(R,G,B) \\
H=\begin{cases}\dfrac{(G-B)}{(V_{\max}-V_{\min})^{36}60} & if\ R=V_{\max} \\ \dfrac{120+(B-R)}{(V_{\max}-V_{\min})^{360}} & if\ G=V_{\max} \\ \dfrac{240+(R-G)}{(V_{\max}-V_{\min})^{360}} & if\ B=V_{\max}\end{cases} \\
S=\frac{V_{\max}-V_{\min}}{V_{\max}} \\
V=V_{\max}
\end{gathered} \tag{29}$$

3. Optimization of visual effects and messaging in visualization design

3.1. Application of ACE optimization algorithm

The optimized ACE algorithm not only has a good color correction effect, but also has a fast processing speed, which enables it to quickly complete the processing of images in the prevailing multi-core processing environment. Therefore, the optimized algorithm is applied to image processing to make it useful in quality improvement of images with color defects.

3.1.1. Experimental ideas. The most basic application of color balancing is to correct the color of images with color shift, improper exposure, oversaturation or undersaturation. Therefore, the ACE optimization algorithm proposed in this paper is mainly used to achieve automatic correction of different images with color defects. Experiments are carried out by selecting different images for equalization and plotting their grayscale histograms in order to objectively observe the changes in the images.

Gray scale histogram is a function that counts the distribution of gray levels of individual pixel points in an image, it counts the number of pixel points in which a certain gray level appears in the image and characterizes the frequency of occurrence of a certain gray level. Specifically, the horizontal coordinate of the histogram is a series of gray levels, and the vertical coordinate is the number or frequency of pixel points with a certain gray level in the image. The state of the histogram can reflect the nature of the image bright image overall gray level value is higher, so the distribution of its grayscale histogram tends to the side of high gray value, that is, concentrated on the right side of the histogram; low contrast image gray pixel value variation range is small, so its histogram is narrower and concentrated in the middle of the gray level; and brightness darker image most of the grayscale value is small, in the histogram is The darker images have smaller gray values, which is reflected in the histogram as the images are concentrated in the left side of the lower gray values. For images with good contrast, brightness and chromaticity, their histograms occupy all possible gray levels and are more evenly distributed.

The effectiveness of the application of the algorithm in this paper is demonstrated by the equalization effect of experimentally selected images with different color defects. One example each of underexposed, overexposed, and off-color images are selected to specifically analyze the effect of ACE optimization algorithm on image equalization.

3.1.2. Automatic Color Equalization of Images:

1) Underexposed images. The underexposed face image is processed by ACE optimization algorithm, Fig. 4 and Fig. 5 show the original grayscale histogram and the grayscale histogram optimized by this paper's algorithm, respectively.

The dynamic range of the original image is small, the pixel distribution is narrow and concentrated in the dark tone region of the gray scale histogram, and there are almost no pixels in the mid-tone and bright tone, so the image is very dark. After color equalization using the ACE algorithm proposed in this paper, not only the desired processing time is obtained, but also the pixel values are significantly expanded and the image saturation is enhanced and clearly visible.

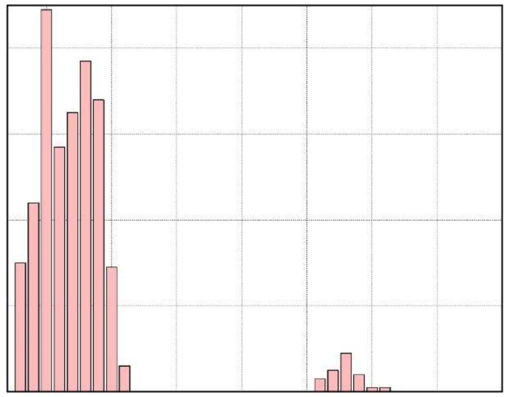

Fig. 4. The exposure is not the original histogram

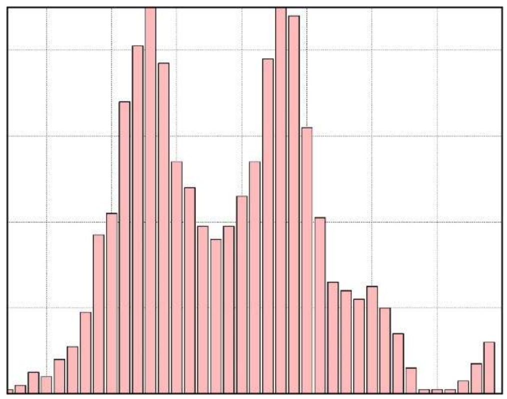

Fig. 5. Optimized histogram

2) Overexposed images. The sunlight image in overexposure case is processed by ACE optimization algorithm, Fig. 6 and Fig. 7 show the original grayscale histogram and the grayscale histogram optimized by this paper's algorithm, respectively.

Since the original image is overexposed, the dynamic range of the original image is small, the pixels are concentrated in the bright tone region of the gray scale histogram, and there are almost no pixels in the dark tone, so the image is very bright with low contrast. After using the optimized ACE algorithm for aggressive color equalization, the processing time is fast and the equalized grayscale histogram extends to almost the entire range of the image grayscale allowable, with a more uniform distribution of grayscale values. The intuitive effect is that the image with increased contrast shows a better sense of brightness and visual effect.

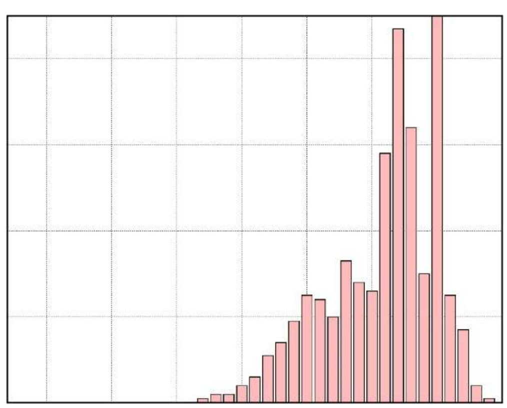

Fig. 6. The exposure is not the original histogram

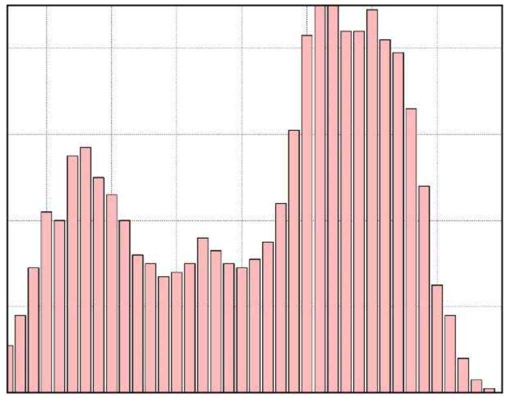

Fig. 7. Optimized histogram

3) Partial color image. Tableware images with the presence of off-color phenomenon are processed by the ACE optimization algorithm, and Fig. 8 and Fig. 9 show the original grayscale histogram and the grayscale histogram optimized by the algorithm of this paper, respectively.

Since the intuitive visual effect of the original image is yellowish, the dynamic range of the image is small, the pixels are concentrated in the mid-tone region, and there are almost no pixels in the bright tone. With the optimized ACE algorithm in this paper, the grayscale histogram of the image is faster and the automatic color equalization extends the range of the image to more gray levels, and the color tone of the image is more natural.

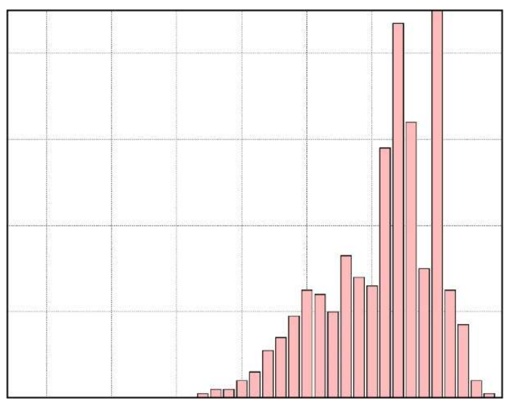

Fig. 8. The exposure is not the original histogram

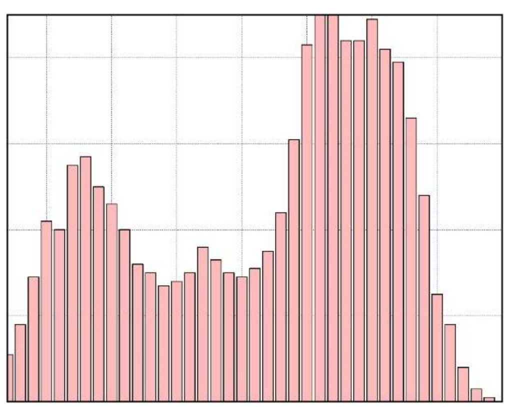

Fig. 9. Optimized histogram

3.2. Visual Effects Enhancement Analysis Based on Robust Principal Component Analysis

3.2.1. Experimental data set. The experimental dataset is the UIEB public dataset. The dataset contains a large number of underwater images, which are mainly divided into two subsets 890 original underwater images and corresponding high quality reference images. 60 challenging underwater images.

3.2.2. Experimental configuration. The computer configuration used for the experiments is as follows: Intel(R) Core(TM) i9-12700H @ 2.70 GHz CPU, 32 GB of RAM.NVIDIA Ge Frceo RTX 3060 Laptop GPU, with a memory size of 6 Gi B. Windows 11, 64-bit operating system. Compiler is Python 3.7.

3.2.3. Quality evaluation measures. The underwater image quality evaluation indexes used in this paper are categorized into full reference image quality evaluation indexes and no reference image quality evaluation indexes.

1) Full reference image quality evaluation index. Mean square error (MSE) is the absolute difference between two images by directly comparing each pixel position, so as to obtain the final total average difference. The smaller the MSE value, the more similar the two images.

Peak Signal to Noise Ratio (PSNR) is a metric that represents the ratio of the maximum possible power of a signal to the power of the destructive noise that affects the accuracy of its representation. The larger the PSNR is, the less distortion there is and the better the quality of the resulting image.

Structural similarity (SSIM) is a metric that measures the similarity between two images in terms of structure and texture.The larger the SSIM, the more similar the structure and texture of the enhanced image is to the reference image.

2) Quality evaluation indexes for reference-free images. In this paper, the following four types of reference-free image quality evaluation indexes are adopted for assessment.

(1) The reference-free image spatial quality evaluator (BRIS-QUE), the natural image quality evaluator (NIQE), and the perception-based image quality evaluator (PIQE), which can evaluate the image sharpness, noise, artifacts, and overall quality. The higher the score value, the lower the image quality.

(2) Average Gradient (AG) can be used to measure the clarity of the fused image. The larger the AG value, the better the image clarity. (c) Spatial frequency (SF) reflects the rate of change of the gray scale of the image, the larger the SF value, the higher the image quality. Standard deviation (STD) is an objective evaluation index to measure the richness of image information, the larger the STD value, the more information the image carries, the better the image quality.

(3) The Tenengrad function uses the Sobel operator to extract the gradient in the horizontal and vertical directions respectively, the larger the value of the Tenengrad gradient function, the sharper the edges of the image are, the Laplacian function replaces the Sobel operator by the Laplacian operator, the Variance function calculates the gray scale difference of an image to evaluate the sharpness of the focused image, the larger the value is, the better the image quality is, the more information the image carries. Entropy entropy function is an important index to measure the richness of image information, the larger the value of Ent, the richer the image.

(4) Underwater Color Image Quality Evaluation (UCIQE) quantitatively evaluates the linear combination of chromaticity, saturation and contrast to quantify uneven color cast, blurring and low contrast, respectively. The higher the value of UCIQE, the better the image quality. Underwater Image Quality Metrics (UIQM) adopts Color Measurement Metrics (UICM), Sharpness Measurement Metrics (UISM) and Contrast Measurement Metrics (UICon M) as the basis of evaluation. The larger the value, the better the color balance, sharpness and contrast of the image.

3.2.4. Experimental results. Using the UIEB dataset, 11 state-of-the-art underwater image enhancement methods (UDCP, GC, CLAHE, IBLA, MSRCR, MIP, RGHS, SeaThru, UCM, WB, ULAP) and the algorithms designed in this paper were compared and analyzed. The experiment treats 890 high-quality reference images in the dataset as underwater images with ground truth images for full reference image comparison evaluation, and the comparison results are shown in Table 1. ↑ indicates that the larger the value the better the effect, and ↓ indicates that the smaller the value the better the effect.

From the results, it can be seen that the algorithm of this paper obtains the optimal performance in the full reference image quality evaluation. The mean square error of 0.6206 is the lowest among all models, and the PSNR and SSIM are 21.1444 and 0.8769, respectively, which are the highest among the models.

Table 1. Results of full-reference image quality evaluation

Method	MSE/10^3 ↓	PSNR ↑	SSIM ↑
UDCP	3.0912	13.555	0.5863
GC	2.6264	14.2597	0.6069
CLAHE	0.6685	20.1031	0.8569
IBLA	0.9687	19.5815	0.7564
MSRCR	1.3588	17.1534	0.7151
MIP	1.344	17.2348	0.7303
RGHS	1.356	17.135	0.7009
Sea Thru	2.15	17.1164	0.7492
UCM	1.2394	17.536	0.7509
WB	0.776	19.905	0.771
ULAP	1.8657	15.774	0.6466
This model	0.6206	21.1444	0.8769

The quality assessment was performed using the reference-free image quality evaluation indexes described above. The results of the four types of evaluation metrics are shown in Tables 2 to 5, respectively.

Table 2 shows the performance of BRISQUE, NIQE and PIQE metrics. The model in this paper is 30.6074, 15.7277, and 21.256 on the three indicators, which is higher than all the rest of the models except the reference image.

Table 2. Results of BRISQUE, NIQE and PIQE

Method	BRISQUE ↓	NIQE ↓	PIQE ↓
UDCP	37.0543	16.095	29.7153
GC	36.044	17.2862	28.4154
CLAHE	34.9093	17.8264	26.3633
IBLA	36.8344	16.3781	29.374
MSRCR	36.3949	16.0248	24.1252
MIP	37.4042	16.8376	28.697
RGHS	34.2869	16.7582	27.3631
Sea Thru	36.6512	17.2278	28.6471
UCM	33.9075	17.1412	25.7046
WB	34.9741	16.9838	27.4175
ULAP	35.6591	17.0825	28.3542
Reference image	20.8135	16.6306	22.1625

This model	30.6074	15.7277	21.256

Table 3 shows the performance of the indicators of mean gradient, spatial frequency and standard deviation. The scores of this paper's model on the three indicators are 8.7111, 18.7503, and 69.2616, respectively.

Table 3. Results of AG, SF and ST

Method	AG ↑	SF ↑	STD ↑
UDCP	3.6786	8.2314	33.5715
GC	3.4876	7.3635	33.175
CLAHE	6.2896	12.9801	46.5322
IBLA	4.6306	10.7401	46.5449
MSRCR	4.2511	9.1391	41.8419
MIP	4.568	10.3459	45.7245
RGHS	5.4162	11.8553	54.5663
Sea Thru	5.2243	11.2944	57.4372
UCM	6.1571	13.0871	54.3014
WB	4.4744	8.5119	35.684
ULAP	4.7873	10.4222	47.7118
Reference image	8.3869	18.0501	67.3334
This model	8.7111	18.7503	69.2616

Table 4 shows the results of UCIQE and UIQM image quality evaluation. The algorithm in this paper is 0.4648 and 0.7577 on the two metrics, ranking first among all algorithms.

Table 4. Results of UCIQE and UIQM

Method	UCIQE ↑	UIQM ↑
UDCP	0.4535	0.6672
GC	0.3306	0.3887
CLAHE	0.4057	0.6905
IBLA	0.4725	0.565
MSRCR	0.4433	0.6324
MIP	0.4186	0.5898
RGHS	0.468	0.7192
Sea Thru	0.4642	0.7554
UCM	0.4546	0.7045
WB	0.4161	0.599
ULAP	0.4473	0.6158
Reference image	0.4429	0.738
This model	0.4648	0.7577

Table 5. Results of Tenengrad, Laplacian, Variance and Entropy

Method	Tenengrad ↑	Laplacian ↑	Variance ↑
UDCP	21.1577	163.3998	3.1975
GC	16.9574	104.8825	3.1407
CLAHE	30.1264	305.1734	5.8373
IBLA	28.9241	214.4506	6.0471
MSRCR	21.2557	147.757	4.74
MIP	23.6525	236.2219	6.2322
RGHS	27.4862	240.6346	6.7753
Sea Thru	27.4285	143.3122	6.9764
UCM	29.6436	344.6272	6.811
WB	20.0272	180.699	3.5236
ULAP	24.0579	206.8732	6.3686
Reference image	37.6782	810.3772	7.7273
This model	37.7853	655.742	7.9607

From Table 2 to Table 5, it can be seen that the scores obtained by the EFUIE algorithm proposed in this paper are close to the scores of the reference image, especially in Tables 3 and 4, which are even higher than the scores of the reference image, which confirms the superiority of the algorithm in this paper even more.

3.3. Analysis of the effectiveness of the message

The algorithm designed in this paper is applied to generate suggestions for sensory elements and apply them in a way that unfolds with physical design.

On the basis of visual process design based on perceptual engineering, a city tourism brochure is redesigned. Based on the skeleton of Zhongshan Bridge and Waterwheel Garden, which are famous attractions in Chengguan District, the brochure is designed to meet the needs of consumers.

Produce a Questionnaire on Consumer Reading Information, which includes the degree of misinterpretation of information, the length of time spent searching for information, the medium of information dissemination, the ratio of text to images, the type of information, and the reading habits of consumers. Figure 10 shows the results of the survey. By analyzing the time consumers spend searching for information it was found that search time, i.e., search efficiency, is the main data for measuring the efficiency of information reading carried out by consumers. If the search time is shorter, it means the information access efficiency is higher, and vice versa. Through the questionnaire, it can be understood that there are many reasons that affect the efficient reading of information. For example, if the layout information meets the psychological needs of consumers, they will actively read and search for effective information; there is also the layout of the graphics, text layout, etc.; the same information conveyance medium also affects the acquisition of information, such as floating advertisements will affect the accuracy of consumers to read the information.

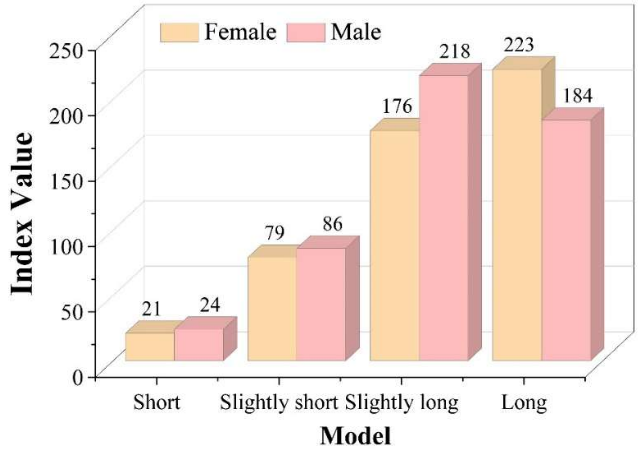

Fig. 10. Consumer search information length scale

In order to promote the efficiency of consumers' reading information, designers need to pay constant attention to consumers' perceptual information in the environment of information redundancy, and by analyzing and organizing it, so that designers what type of information and how to layout meet the needs of consumers. The correctness of the perception of the consumer's senses in visual communication design depends on the efficiency of retrieving mental representations in the consumer's memory, and it also has an important impact on the designer's interpretation of consumer cognition and behavior. Therefore, on the basis of understanding consumption, it is also necessary to popularize the relevant knowledge to improve the correctness of consumer cognition. Perceptual engineering makes a necessary addition to the field of studying visual communication design, which helps to communicate information efficiently and accurately in the future.

4. Conclusion

In this paper, based on the retina-cortex theory, we propose a visual effect-oriented automatic color equalization method, and further design an adaptive visual enhancement algorithm based on Robust Principal Component Analysis (RPCA), which is used to assist in optimizing the visual effect and information communication in visual design. The performance of the algorithm is examined on the dataset by applying full-reference and no-reference image quality evaluation metrics. It is found that for underexposed images, the color equalization performed by this paper's algorithm not only obtains the desired processing time, but also the pixel values are significantly expanded, and the image saturation is enhanced and clearly visible. In the full reference image quality evaluation, this paper's algorithm obtains the optimal performance, with the lowest mean square error of 0.6206 among all the models, and the PSNR and SSIM of 21.1444 and 0.8769, respectively, which are the highest among the models. The average gradient, spatial frequency, and standard deviation scores are 8.7111, 18.7503, and 69.2616, leading the rest of the baseline models, and the algorithm meets the design expectations.

References

[1] Bian, J., & Ji, Y. (2021). Research on the teaching of visual communication design based on digital technology. Wireless Communications and Mobile Computing, 2021(1), 8304861.

[2] Zhang, Z., Gao, Y., Zhou, S., Zhang, T., Zhang, W., & Meng, H. (2022). Psychological cognitive factors affecting visual behavior and satisfaction preference for forest recreation space. Forests, 13(2), 136.

[3] LANA, J., & WANLI, C. (2021). An analysis of the characteristics of cross-media photography based on visual communication design. language, 3(2), 30-34.

[4] Gao, Y., Wu, L., Shin, J., & Mattila, A. S. (2020). Visual design, message content, and benefit type: the case of a cause-related marketing campaign. Journal of Hospitality & Tourism Research, 44(5), 761-779.

[5] Jeffrey Okun, V. E. S., & Susan Zwerman, V. E. S. (Eds.). (2020). The VES handbook of visual effects: industry standard VFX practices and procedures. Routledge.

[6] Camargo, M. C., Barros, R. M., & Barros, V. T. (2018, April). Visual design checklist for graphical user interface (GUI) evaluation. In proceedings of the 33rd annual ACM symposium on applied computing (pp. 670-672).

[7] Park, S. H., Lee, P. J., Jung, T., & Swenson, A. (2020). Effects of the aural and visual experience on psycho-physiological recovery in urban and rural environments. Applied Acoustics, 169, 107486.

[8] Ledford, J. R., Lane, J. D., & Severini, K. E. (2018). Systematic use of visual analysis for assessing outcomes in single case design studies. Brain Impairment, 19(1), 4-17.

[9] Jaenichen, C. (2017). Visual communication and cognition in everyday decision-making. IEEE computer graphics and applications, 37(6), 10-18.

[10] Skliarenko, N. V., Gryshchenko, I., & Kolosnichenko, M. V. (2021). Symmetry in the visual communication design: methods of dynamic image construction. Art and design.

[11] Murchie, K. J., & Diomede, D. (2020). Fundamentals of graphic design—essential tools for effective visual science communication. Facets, 5(1), 409-422.

[12] Rose, G. (2022). Visual methodologies: An introduction to researching with visual materials. sage.

[13] Weber, W., & Rall, H. M. (2022). The Semiotic Work Design Can Do: A Multimodal Approach to Visual Storytelling. In Periodical Studies Today (pp. 187-204). Brill.

[14] Dronova, I. (2017). Environmental heterogeneity as a bridge between ecosystem service and visual quality objectives in management, planning and design. Landscape and Urban Planning, 163, 90-106.

[15] Garcia-Retamero, R., & Cokely, E. T. (2017). Designing visual aids that promote risk literacy: A systematic review of health research and evidence-based design heuristics. Human factors, 59(4), 582-627.

[16] Williams, W. R. (2019). Attending to the visual aspects of visual storytelling: using art and design concepts to interpret and compose narratives with images. Journal of Visual Literacy, 38(1-2), 66-82.

[17] Yue, W. (2020, May). Research on innovative application of new media in visual communication design. In Journal of Physics: Conference Series (Vol. 1550, No. 3, p. 032146). IOP Publishing.

[18] Guo, D., McTigue, E. M., Matthews, S. D., & Zimmer, W. (2020). The impact of visual displays on learning across the disciplines: A systematic review. Educational Psychology Review, 32(3), 627-656.

[19] Lee, P. S., West, J. D., & Howe, B. (2017). Viziometrics: Analyzing visual information in the scientific literature. IEEE Transactions on Big Data, 4(1), 117-129.

[20] Qu, Y., Chen, Y., Huang, J., & Xie, Y. (2019). Enhanced pix2pix dehazing network. In Proceedings of the IEEE/CVF conference on computer vision and pattern recognition (pp. 8160-8168).

[21] Bowen, A. (2018). The visual effect: a literature review of visual design principles as they apply to academic library websites. Internet Reference Services Quarterly, 23(3-4), 67-88.

[22] Soomro, Y. A., Kaimkhani, S. A., & Iqbal, J. (2017). Effect of visual merchandising elements of retail store on consumer attention. Journal of business strategies, 11(1), 21-40.

[23] Forceville, C. (2020). Visual and multimodal communication: Applying the relevance principle. Oxford University Press.

[24] Shi, Y., Liu, P., Chen, S., Sun, M., & Cao, N. (2022). Supporting expressive and faithful pictorial visualization design with visual style transfer. IEEE Transactions on Visualization and Computer Graphics, 29(1), 236-246.

[25] Kuo, L., Chang, T., & Lai, C. C. (2022). Multimedia webpage visual design and color emotion test. Multimedia Tools and Applications, 81(2), 2621-2636.

[26] Cho, J. Y. (2017). An investigation of design studio performance in relation to creativity, spatial ability, and visual cognitive style. Thinking Skills and Creativity, 23, 67-78.

[27] Isenberg, P., Lee, B., Qu, H., & Cordeil, M. (2018). Immersive visual data stories. Immersive analytics, 165-184.

[28] Seifert, C., & Chattaraman, V. (2020). A picture is worth a thousand words! How visual storytelling transforms the aesthetic experience of novel designs. Journal of Product & Brand Management, 29(7), 913-926.

[29] Kim, H., Lee, M., Kim, G. J., & Hwang, J. I. (2021). The impacts of visual effects on user perception with a virtual human in augmented reality conflict situations. IEEE Access, 9, 35300-35312.

[30] Tomita, K. (2022). Visual design as a holistic experience: How students' emotional responses to the visual design of instructional materials are formed. Educational technology research and development, 70(2), 469-502.

[31] Liu, W., Cao, Y., & Proctor, R. W. (2021). How do app icon color and border shape influence visual search efficiency and user experience? Evidence from an eye-tracking study. International Journal of Industrial Ergonomics, 84, 103160.

[32] Tong, X., Chen, Y., Zhou, S., & Yang, S. (2022). How background visual complexity influences purchase intention in live streaming: The mediating role of emotion and the moderating role of gender. Journal of Retailing and Consumer Services, 67, 103031.

[33] Jongmans, E., Jeannot, F., Liang, L., & Dampérat, M. (2022). Impact of website visual design on user experience and website evaluation: the sequential mediating roles of usability and pleasure. Journal of Marketing Management, 38(17-18), 2078-2113.

[34] Bresciani, S. (2019). Visual design thinking: A collaborative dimensions framework to profile visualisations. Design Studies, 63, 92-124.

[35] Bylinskii, Z., Kim, N. W., O'Donovan, P., Alsheikh, S., Madan, S., Pfister, H., ... & Hertzmann, A. (2017, October). Learning visual importance for graphic designs and data visualizations. In Proceedings of the 30th Annual ACM symposium on user interface software and technology (pp. 57-69).

[36] Shinahara, Y., Karamatsu, T., Harada, D., Yamaguchi, K., & Uchida, S. (2019, September). Serif or sans: Visual font analytics on book covers and online advertisements. In 2019 International Conference on Document Analysis and Recognition (ICDAR) (pp. 1041-1046). IEEE.

[37] Chen, M., & Ebert, D. S. (2019, June). An ontological framework for supporting the design and evaluation of visual analytics systems. In Computer Graphics Forum (Vol. 38, No. 3, pp. 131-144).

[38] Yu Luo,Guoliang Lv,Jie Ling & Xiaomin Hu.(2024).Low-light image enhancement via an attention-guided deep Retinex decomposition model.Applied Intelligence(2),194-194.

[39] Lingaiah Jada,Rangu Srikanth & Kalagadda Bikshalu.(2024).Effective low-exposure color image enhancement based on histogram equalization with spatial contextual information.Engineering Research Express(4),045236-045236.

[40] Qile Zhu,Shiqian Wu,Shun Fang,Qi Wu,Shoulie Xie & Sos Agaian.(2024).Fast tensor robust principal component analysis with estimated multi-rank and Riemannian optimization.Applied Intelligence(1), 52-52.

[41] Sharanabasav Hosamani & Shashidhar Sonnad.(2025).Image quality enhancement using optimized thresholding and two-level diffusion-based denoising filter.The Imaging Science Journal(2),245-265.